Effects of beam focusing on the efficiency of planar waveguide grating couplers

Lifeng Li and Mool C. Gupta

Results of a theoretical and experimental investigation into the variation of coupling efficiency with coupling angle are presented for various beam focusing conditions for an integrated optical grating coupler. This investigation shows that the acceptance angle of the grating coupler can be broadened, over a very large range and with a relatively small loss of coupling efficiency, by focusing the incident beam onto the grating.

Key words: Integrated optics, grating couplers

I. Introduction

Diffraction gratings play an important role in integrated optics: they are used to couple light into waveguides; to focus, deflect, and split beams; and to filter light spectrally (as in distributed feedback lasers).[1,2] Grating couplers are not only durable, they can be fabricated through planar photolithographic techniques.

A distinctive feature of a periodic grating coupler is that its coupling efficiency is high only if the incident beam falls within a narrow range of coupling angles.[3] In many cases this feature can be used to some advantage. For some applications, however, it is desirable to render the coupling efficiency less sensitive to the coupling angle. One way to achieve this is by focusing the incident beam. A focused beam can be considered a bundle of rays with a range of angular components. When this angular range covers the optimum coupling angle, a portion of the bundle will be coupled into the waveguide and the remainder will not. Thus, the curve of coupling efficiency vs coupling angle will be broadened, but its peak height will be lowered.

Even though grating couplers are widely used in integrated optics, and even though the theory of grating couplers is well understood, to our knowledge little detailed study has been done on the angular dependence of the coupling efficiency for focused beams. In this paper we report the results of our theoretical and experimental investigation into the variation with coupling angle of the coupling efficiency for an integrated optical grating coupler. Various focused beam conditions were explored in our investigation. The important question we address is how great an angular broadening can be achieved for a given loss of peak efficiency.

II. Theory

The analysis of a grating coupler requires two calculations: (1) the calculation of the effective index and leakage factor of the corrugated waveguide, and (2) the calculation of the coupling efficiency. For the first calculation we use Maystre's integral method.[4] For the second calculation we use the method developed by Neviere et al.[5-8] This method consists of three steps. First, an incident beam of finite width is represented by a superposition of plane waves. Second, the response of the grating coupler for a plane wave in the vicinity of the waveguide resonance is represented by a complex pole. Third, the total response of the coupler to the finite beam is given by the superposition of its response to plane waves. Neviere et al.[7] considered only the case in which the incident angle is phase matched with the grating coupler, and the incident beam has no phase variation other than that of a plane wavefront. In our work we considered the general case. By allowing an arbitrary incident angle and arbitrary phase variation, we studied the angular dependence and defocus dependence of the device's coupling characteristics. Throughout this paper we assume that $l \gg 1/\alpha'$, where l is the grating length and α' is the leakage factor defined below. This condition is well satisfied by the grating couplers used in our experiment.

Following the analysis in Refs. 7 and 8, one can

derive the following expression for the coupling effi-
ciency for a lossless, infinitely long grating coupler:

$$\eta(x) = \frac{1}{\ldots} \quad \ldots = mK \ldots$$

$$+ \text{Re} \ldots \ldots \quad (1)$$

where x is the position along the grating and y is
measured along the normal to the waveguide; $k_0 = 2\pi$
λ, with λ the wavelength in a vacuum; n is the refractive
index of the incident medium; $C(y) = 1$ for TE, and
$C(y) = 1\,\epsilon$ for TM, with ϵ the dielectric constant, and C
is $C(y)$ in the incident medium; $\alpha = k_0 N_{eff}$, with N_{eff} the
effective index of the guided mode; $K = 2\pi/d$, with d
the grating period; m is the diffraction order which gets
coupled into the waveguide; v_m is the mth order field
amplitude excited by an incident plane wave on reso-
nance; and $q(x)$ gives the incident beam profile, nor-
malized such that $\int q^2 dt = 1$, with t perpendicular to
the beam axis.

The variables defined above are properties of the
grating coupler and of the incident beam. The inter-
action between the coupler and the incident beam is
described completely by the function $r(x)$, which can
be stated in three equivalent forms:

$$\frac{dr(x)}{dx} + i(\alpha_0 - \alpha)r(x) = q(x), \qquad (2)$$

$$r(x) = -i \int p(\xi) \frac{1}{\xi + \alpha_0 - \alpha_p} \exp(i\xi x)\, d\xi, \qquad (3)$$

$$r(x) = \int q(x')H(x - x') \exp[i(\alpha_0 - \alpha)(x - x')]\, dx'. \qquad (4)$$

where $p(\xi)$ is the Fourier transform of $q(x)$; $\alpha_0 = nk_0$
$\sin \theta_0$ is the center spatial frequency of $p(\xi)$; θ_0 is the
incident angle; $\alpha_p = nk_0 \sin\theta_R + i\alpha'$ is the complex pole
of the waveguide grating structure; θ_R is the resonance
coupling angle; α' is the leakage factor; and $H(x - x') =$
1 if $x - x' > 0$ and $H(x - x') = 0$ if $x - x' < 0$. Equation
(2) is probably the most useful for a numerical compu-
tation of $r(x)$, but Eqs. (3) and (4) are more useful for
an intuitive understanding of the dependence of $r(x)$
on the incident angle or beam size (angular width) of
the incident beam. We define several terms to simpli-
fy our discussion. $\Theta \equiv \theta_0 - \theta_R$, the angular detuning.
We define the full width at half maximum of the η vs Θ
curve, the apparent acceptance angle (or, simply, the
acceptance angle) of the grating coupler, and denote
this by $\Delta\theta_a$. Clearly, $\Delta\theta_a$ depends both on the grating
coupler and on the incident beam. It can be shown[3]
that, as the incident beam becomes a plane wave, $\Delta\theta_a$
tends to its lowest value $\Delta\theta_i = 2\,\text{Im}[\alpha_p]/(nk_0\cos\theta_R)$,
which is the full width at half-maximum of the Lorent-
zian profile $|1/(\xi + \alpha_0 - \alpha_p)|^2$. We call $\Delta\theta_i$ the intrinsic
acceptance angle of the grating coupler.

The angular dependence of $\eta(x)$ is contained in the
function $r(x)$. When $\Theta = 0$, $r(x)$ as given by Eq. (4) is a
convolution of the incident beam profile and an expo-
nential decay function. When $\Theta \neq 0$, an oscillatory
function is superimposed on the exponential decay
function; therefore, the coupling efficiency decreases.
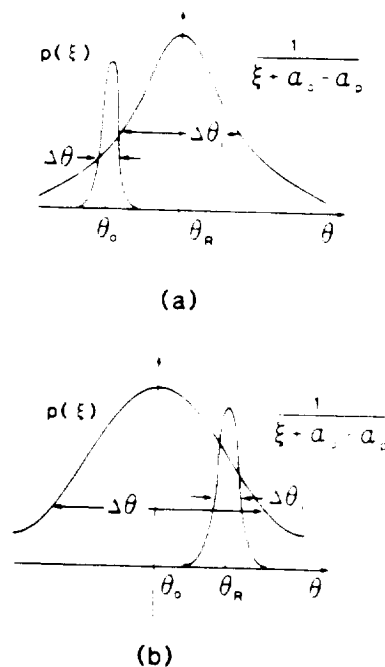In Eq. (3), $r(x)$ is given by an overlapping integral of

(a)

(b)

Fig. 1. Two limiting cases for the overlap integral given in Eq.
(a) $\Delta\theta \ll \Delta\theta_i$ and (b) $\Delta\theta \gg \Delta\theta_i$.

$p(\xi)$ and $1/(\xi + \alpha_0 - \alpha_p) \exp(i\xi x)$. When $\Theta = 0$, the
peaks of the two functions coincide, and the maximum
coupling efficiency is achieved. A nonzero detuning
implies a shift in the two peaks and a decrease in
efficiency. When Θ changes, the two curves move
relative to each other. If the angular width of incident
beam $\Delta\theta$ is $\ll\Delta\theta_i$, the Lorentzian is probed by the
incident beam; if $\Delta\theta$ is $\gg\Delta\theta_i$, the incident beam is
probed by the Lorentzian (Fig. 1). In other words, the
apparent acceptance angle approaches the intrinsic
acceptance angle as $\Delta\theta$ tends to zero, and it approaches
$\Delta\theta$ as the latter becomes $\gg\Delta\theta_i$.

Now let us consider a Gaussian beam, as depicted in
Fig. 2. Once the wavelength and polarization are
known, a Gaussian beam is specified completely by its
beam waist ω_0 or its angular width $\Delta\theta$. These two
quantities are related by $\Delta\theta = \tan^{-1}(\lambda/\pi\omega_0)$. For our
purposes it is more convenient to use the angular
width. To specify the position of a Gaussian beam
relative to a grating coupler we need three parameters:
incident angle θ_0, lateral offset x_0, and defocus z_0. The
lateral offset is defined as the distance between the
beam axis and the edge of the grating. The defocus is
defined as the distance between the beam's center on
the grating to the beam waist, as shown in Fig. 2. We
consider only the angular dependence, and we set $z_0 =$
0. We consider the influence of defocus on the cou-
pling efficiency at a later time.

III. Experimental Procedures

The optical waveguide was prepared by e-beam de-
position[9,10] of a Corning 7059 glass film onto a quartz
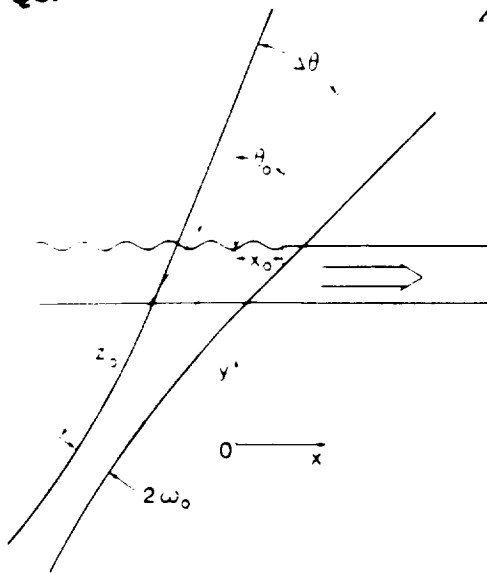substrate with refractive index 1.46. The thin film

Fig. 2.   Geometric configuration for optical coupling of a Gaussian beam by a grating coupler.

Fig. 3.   Theoretical coupling efficiency vs coupling angle for four different Gaussian beam angular widths.

was 0.6 μm thick, its refractive index was 1.50, and its optical loss was 1 dB/cm. The waveguide cover is air. For TE polarization this waveguide supports only the lowest order guided mode. A surface relief grating was etched into the film at the air–film interface. The grating was fabricated by the holographic technique. A 0.22-μm thick photoresist (Shipley 1400 series) thin film was spin coated onto the quartz substrate. The resist was exposed with interference fringes 0.38 μm apart (using a He–Cd laser with a wavelength of 0.4416 μm). The exposed grating pattern was then developed, with an *in situ* monitoring technique.[11] The relief pattern was transferred to the 7059 glass waveguide by reactive ion beam etching with a C_2F_6 gas. The ion beam etch rate for the film was found to be 15 nm/min at an ion beam current density of 1 mA/cm². The shape of the grating rulings was rectangular. From a comparison of the measured and theoretically calculated diffraction efficiencies at several incident angles, we estimated that the grating groove had a depth of 0.17 μm. Two gratings, each 5 mm long, were etched ~2 cm apart on a single sample, one grating to be used as the input coupler and the other as the output coupler.

The angular measurements were taken by mounting the grating coupler on a rotation stage with a 0.001° resolution. Intensities of the transmitted, reflected, and throughput beams were measured with silicon detectors. The detector for the reflected signal had a large receiving area, so that the reflected beam would remain on the detector during the entire measurement process. The coupling efficiency measurements were performed with a polarized He–Ne laser with a Gaussian beam profile. The laser beam was expanded and nearly collimated, so that its angular halfwidth was 0.0085°, corresponding to a 2.7-mm diam beam waist. To obtain other angular widths, convex lenses of vari-
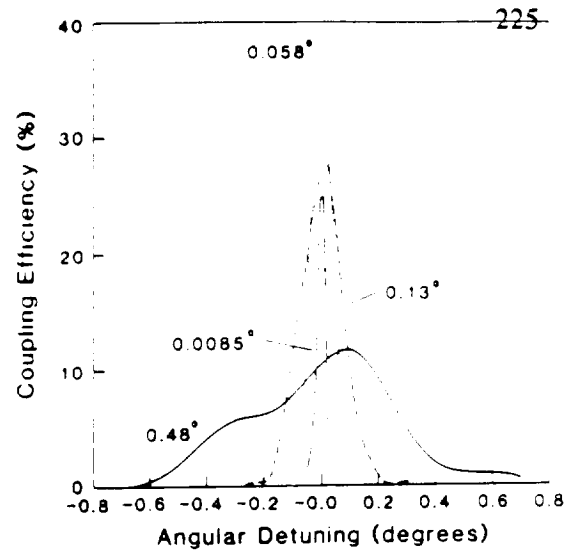
ous focal lengths were inserted after the beam expander. For all the measurements reported here, the input grating coupler was positioned at the beam waist and the laser beam was TE polarized with respect to the grating coupler.

Each focused beam experiment proceeded as follows: First, the optimum coupling condition was located iteratively by adjusting the lateral offset and the coupling angle, so that the sum of the transmitted and reflected intensities was minimized. Once the optimum condition was obtained, the lateral offset was fixed for the remainder of the measurement, and the coupling angle was referred to as the zero angular detuning. At the beginning of the measurement sequence, the grating was rotated to a negative detuning value at which the coupling efficiency was sufficiently low. The grating was then rotated, in small increments, in the positive direction until the coupling efficiency was sufficiently low at a positive detuning value. The transmitted and reflected light intensities were measured at each angular position, from which the coupling efficiency was calculated.

IV. Results

In Fig. 3, four theoretical curves for coupling efficiency vs angular detuning are plotted. For each curve the angular width of the incident beam is indicated.

Experimental data for variations in the coupling efficiency with coupling angle for four focused beam conditions are shown in Figs. 4–7. The percentage transmission, reflection, and throughput data were obtained. The throughput, that is, the light outcoupled by the second grating, is given in arbitrary units but is directly proportional to the coupling efficiency. The experimental coupling efficiencies were calculated by subtracting the percentage transmission and reflection from one hundred. We expect these coupling efficiency values to be somewhat higher than the actual values, because absorption and scattering are not taken into
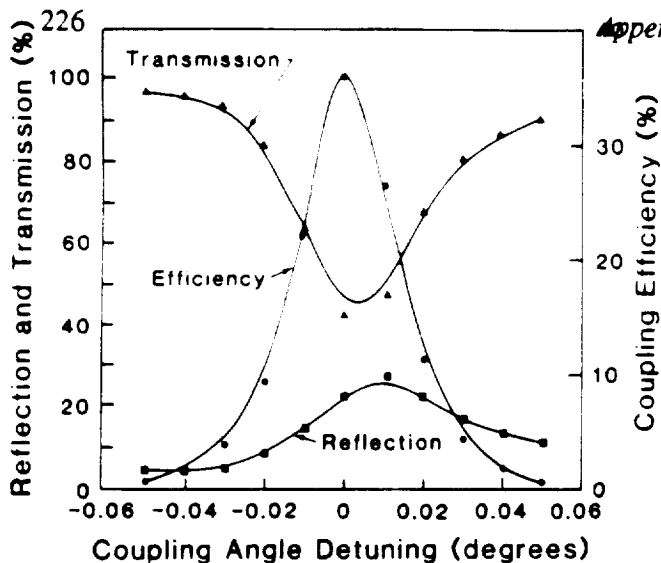
Fig. 4. Experimental data of percentage transmission, reflection, and coupling efficiency vs angular detuning for a Gaussian beam of 0.0085° angular width.
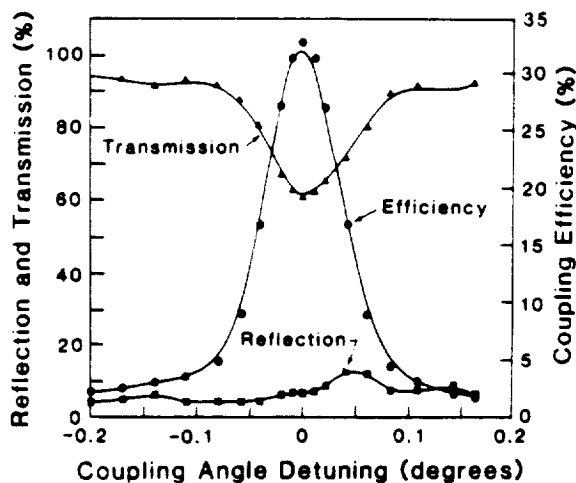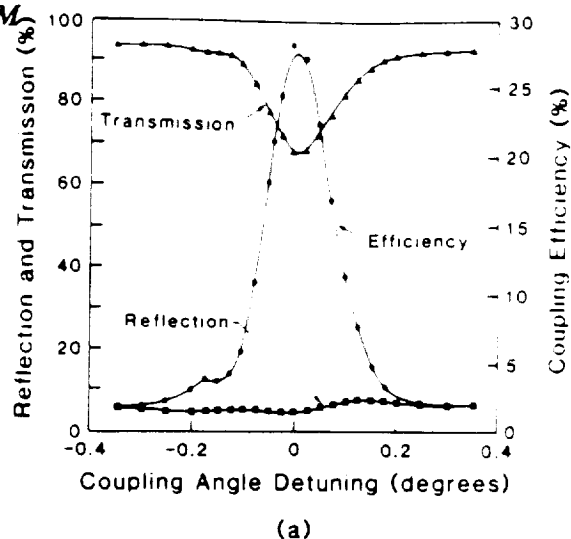

(a)

Fig. 5. Experimental data of percentage transmission, reflection, and coupling efficiency vs angular detuning for a Gaussian beam of 0.058° angular width.

(b)

Fig. 6. Experimental data of (a) percentage transmission, reflection, and coupling efficiency, and (b) outcoupled power vs angular detuning for a Gaussian beam of 0.13° angular width.

account. However, for a study of the angular dependence of the coupling efficiency, this definition suffices.

The experimental values of the transmission, reflection, and coupling efficiency for a Gaussian beam with a 0.0085° angular width are shown in Fig. 4. These values indicate an increase in the transmitted signal and a decrease in the reflected signal as the incident angle is detuned. In addition, the angular position between the transmission minimum and the reflection maximum is shifted. The acceptance angle, measured from the efficiency curve, is 0.029°. Although the peak value of the experimental curve is greater than the theoretical value given in Fig. 3, the acceptance angles measured from both curves agree well.

The experimental data and the theoretical efficiency curves for Gaussian beams with angular widths of

0.058° and 0.13° are shown in Figs. 5 and 6(a), respectively. The shapes of these curves are similar to that of the curve shown in Fig. 4. Note that, although the peak efficiency values are comparable with that in Fig. 4, the apparent acceptance angles have increased to 0.085° and 0.15°, respectively. There is good agreement between the experimental and theoretical curves. The variation in the coupling efficiency with coupling angle, as measured with the outcoupled beam from the second grating, is illustrated in Fig. 6(b). The measured throughput signal curve agrees well with the measured efficiency curve, but the throughput signal has a much higher signal-to-noise ratio.

The experimental transmission, reflection, and coupling efficiency data for a Gaussian beam with a 0.48° angular width are shown in Fig. 7(a). For this case, the
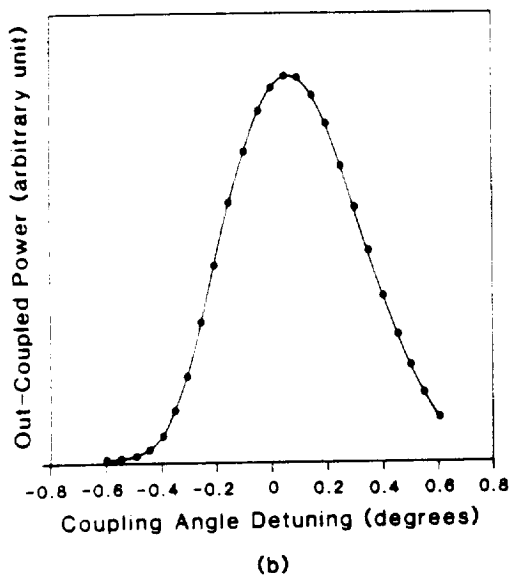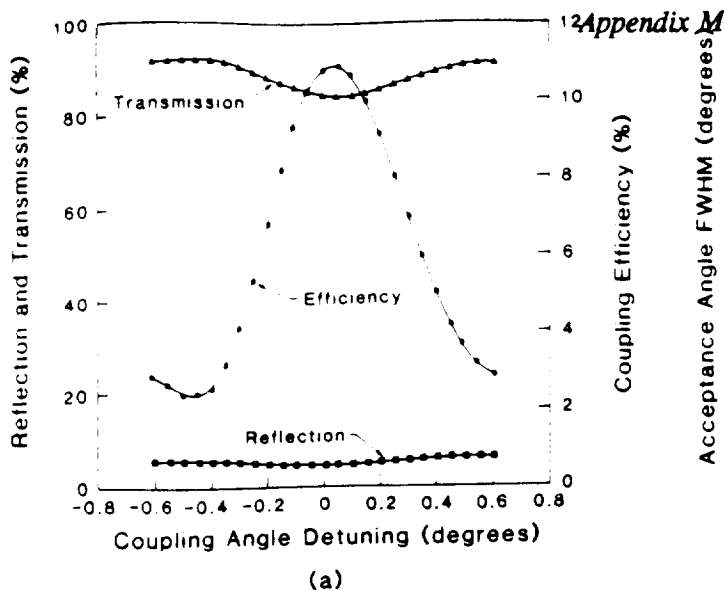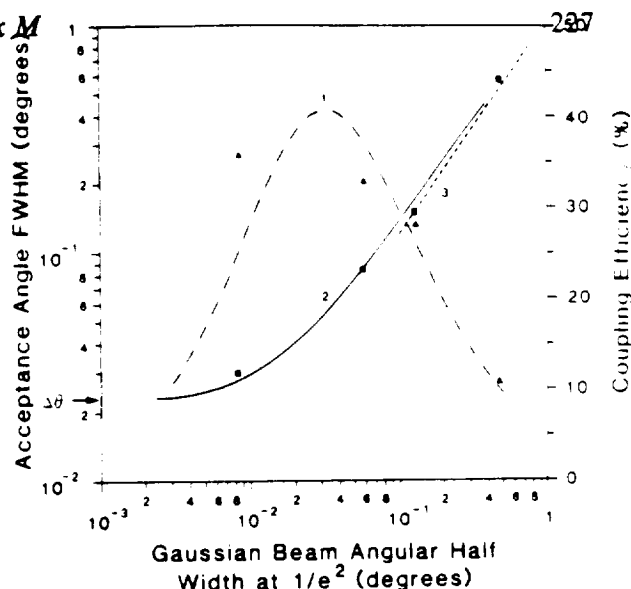
(a)

Fig. 8. Experimental and theoretical acceptance angle (squares and solid line) and coupling efficiency (triangles and long dashed line) vs Gaussian beam angular width.

(b)

Fig. 7 Experimental data of (a) percentage transmission, reflection, and coupling efficiency, and (b) outcoupled power vs angular detuning for a Gaussian beam of 0.48° angular width.

acceptance angle rises to 0.57° and the peak efficiency falls to 11%. The apparent acceptance angle is about twenty times and the peak efficiency about two-thirds that for the beam of 0.0085° angular width. The rise in efficiency around −0.4° detuning arises from substrate mode coupling. A simple calculation shows that, for the grating coupler used in the measurements, the onset coupling angle for the substrate mode is about −0.4° from the optimum coupling angle for the guided mode. Thus, as the coupling angle is detuned in the negative direction, a portion of the input beam is coupled into the substrate. Because of the way we define coupling efficiency, this substrate coupling effect appears in the efficiency curve. No such effect is seen in the beam outcoupled by the second grating [see

Fig. 7(b)]. Likewise, this effect did not appear in our earlier experiments because the acceptance angles were well under 0.4°. It is not known why the shoulder on the left of the theoretical efficiency curve does not appear on the experimental curve. Despite the difference in the shapes of the experimental and theoretical efficiency curves, the acceptance angles measured from these two curves are nearly equal.

V. Discussion and Conclusions

The experimental results and theoretical calculations for the four focused beams are presented in Fig. 8. The horizontal axis is taken as the angular halfwidth of the incident Gaussian beam at $1/e^2$. All the curves and data points share this axis. Curve 1 represents the theoretical coupling efficiency and curve 2 the theoretical apparent acceptance angle; the triangles and squares are the respective experimental points. The arrow indicates the position of the intrinsic acceptance angle $\Delta\theta_i$ of the grating coupler on the vertical axis. Curve 3 shows the calculated relationship between the full width at half-maximum and the halfwidth at $1/e$-maximum for a Gaussian beam. As indicated in Sec. II, as the angular width of the incident beam decreases, the apparent acceptance angle of the grating coupler approaches the intrinsic acceptance angle. Furthermore, as the angular width of the incident beam increases, the apparent acceptance angle approaches the width of the incident beam. Also, at the maximum coupling efficiency, the apparent acceptance angle is about twice the width of the incident beam. Except for two efficiency data points, the experimental data and the theoretical curves are in good agreement.

Note that, in Fig. 8, the coupling efficiency is plotted on a linear scale, while the acceptance angle is plotted on a logarithmic scale. It can be seen that, for a small

loss of efficiency, the acceptance angle can be enlarged several times by using a more tightly focused beam. For example, to achieve the 42% maximum coupling efficiency, one must use a Gaussian beam with a 0.03° angular halfwidth, for which the apparent acceptance angle is ~0.06°. If one is content with a 30% coupling efficiency (~25% less than the maximum value) and wishes to double the acceptance angle, one can do so by focusing the incident beam to an angular halfwidth of 0.1°.

The asymptotic behavior of curve 2 at the lower end suggests that the intrinsic acceptance angle can be probed by a sufficiently collimated beam. Because the intrinsic acceptance angle is directly proportional to the leakage factor for the grating coupler, one could easily measure the leakage factor.

Summarizing, we have conducted a theoretical and experimental study of the angular dependence of the coupling efficiency for a planar waveguide grating coupler. Our results show that, by appropriately focusing the incident Gaussian beam, the acceptance angle of the coupler can be greatly increased with only a small decrease in the maximum coupling efficiency. We also show good agreement between theoretical calculations and experimental measurements. This study allows one to estimate the acceptance angle and coupling efficiency for a grating coupler with a focused incident beam. These findings are useful in applications where the angular tolerance of waveguide coupling is an important issue.

References

1. A. Yariv and M. Nakamura, "Periodic Structures for Integrated Optics," IEEE J. Quantum Electron. QE-13, 233–253 (1977).

2. T. Suhara and H. Nishihara, "Integrated Optics Components and Devices Using Periodic Structures," IEEE J. Quantum Electron. QE-22, 845–867 (1986).

3. K. Ogawa, W. S. C. Chang, B. L. Sopori, and F. J. Rosenbaum, "A Theoretical Analysis of Etched Grating Couplers for Integrated Optics," IEEE J. Quantum Electron. QE-9, 29–42 (1973).

4. D. Maystre, "Integral Methods," in Electromagnetic Theory of Gratings, R. Petit, Ed. (Springer-Verlag, Berlin, 1980), pp. 100.

5. M. Neviere, R. Petit, and M. Cadilhac, "About the Theory of Optical Grating Coupler-Waveguide Systems," Opt. Commun. 8, 113–117 (1973).

6. M. Neviere, P. Vincent, R. Petit, and M. Cadilhac, "Systematic Study of Resonances of Holographic Thin Film Couplers," Opt. Commun. 9, 48–53 (1973).

7. M. Neviere, P. Vincent, R. Petit, and M. Cadilhac, "Determination of the Coupling Coefficient of a Holographic Thin Film Coupler," Opt. Commun. 9, 240–245 (1973).

8. M. Neviere, "The Homogeneous Problem," in Electromagnetic Theory of Gratings, R. Petit, Ed. (Springer-Verlag, Berlin, 1980), pp. 123–157.

9. M. C. Gupta and T. A. Strasser, "Electron-Beam-Deposited Corning 7059 Glass Thin Films for Waveguides," Proc. Soc. Photo-Opt. Instrum. Eng. 993, 44–45 (1988).

10. M. C. Gupta, "Low-Optical-Loss Glass Thin Films," Appl. Opt. 29, 4310–4314 (1990).

11. L. Li, M. Xu, G. I. Stegeman, and C. T. Collin, "Fabrication of Photoresist Masks for Submicrometer Surface Relief Gratings," Proc. Soc. Photo-Opt. Instrum. Eng. 835, 72–82 (1987).